SMALL RING LATTICE PROBLEMS

E.J.N. Wilson
CERN, Geneva, Switzerland

ABSTRACT

This is a review of the special problems in particle dynamics lattice design, and magnet construction and measurement which should be considered in the design of small synchrotrons and storage rings. The CERN Antiproton Accumulator is used as an illustration.

1. INTRODUCTION

This report sets out the practical problems which face the designer of a small storage ring : the CERN Antiproton Accumulator. The designers of other small rings for electrons and high intensity proton synchrotrons will encounter similar problems. Their solutions may differ according to the application but the example will be instructive

Synchrotrons built for the highest energy electrons and protons are built of hundreds and even thousands of small aperture magnets several meters in length. There are usually several hundred regular periods and enough space in the six or eight insertions to string together a series of purpose built sections for injection, ejection, dispersion correction and low beta matching. In a small ring the number of magnets and periods is severely restricted and one must often exercise considerable ingenuity to arrive at a design which satisfies all the requirements necessary to arrive at the desired performance.

The ends of the long high - energy - machine magnets constitute only a small fraction of the integrated field seen by a circulating beam and the fact that the fields in the ends are three - dimensional can usually be ignored. Indeed many of the computer programs developed for the design of large rings contain approximations which treat the magnets as pure, two - dimensional fields and ignore the small curvature of the central trajectory through the end field. Such approximations must be reviewed critically by the designer of a small ring where the magnet aperture can become comparable to the length and where much of the magnet's effect comes from a fringe field in which the particle is deflected with a radius of curvature comparable to the magnet's length.

In this report we first discuss how one may satisfy a number of design constraints in a small ring like the Antiproton Accumulator, how measurement and correction of the end field can be combined with Q measurements on the finished machine to correct effects introduced by short magnets of large aperture, and finally we consider a class of end effects which are not normally included in even the most rigorous lattice programs.

2. THE EXAMPLE – AN ANTIPROTON ACCUMULATOR

In the photograph taken though a "fish - eye" lens, we see the large bending dipoles and focusing quadrupoles of the Antiproton Accumulator which has a mean radius of 25 m. The objects to be seen in Figure 1, wrapped in shiny aluminium bake - out jackets and installed in between some of the magnets are pick - ups and kickers which are mainly used for stochastic cooling and do not concern us for the purposes of this talk.

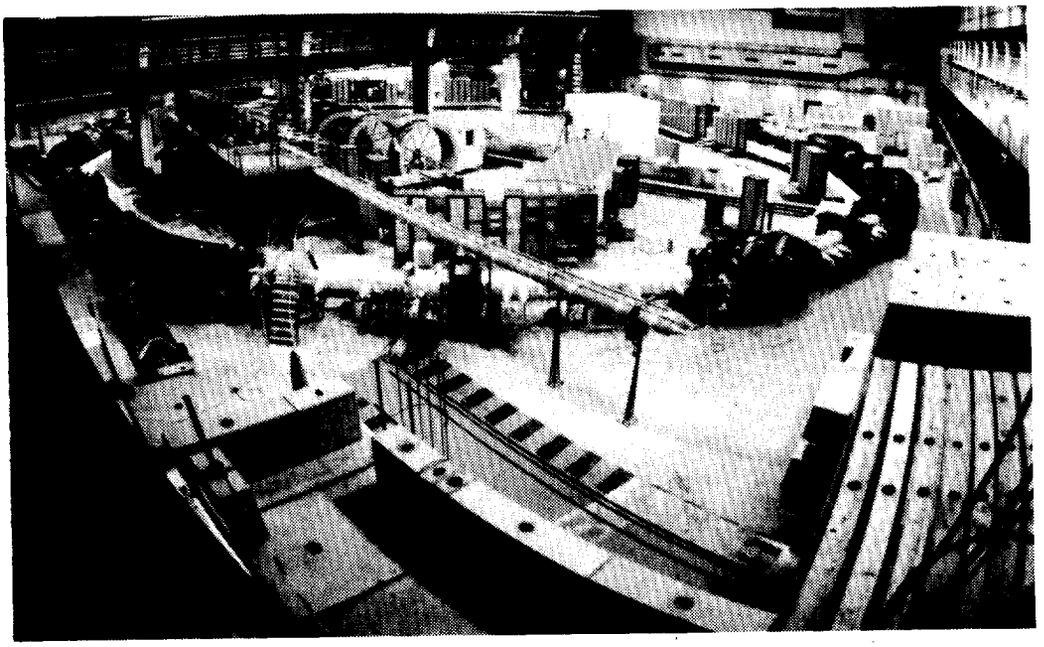

Figure 1: A Fish - eye view of the Antiproton Accumulator

In the bottom right hand corner of the plan view shown in Figure 2, we see the target where antiprotons are produced and a short transport line which brings them to a point, at 12 o'clock on the "dial" of the ring, where they are bent by a septum magnet to join the circulating beam. A little further around, at about 2 o'clock on the dial, is a kicker magnet which inflects them onto the injection orbit. At 10 o'clock is an ejection kicker which uses the same septum to extract the beam which has been accumulated and stored.

One of the constraints on the design is that these kickers should be located at a particular horizontal betatron phase advance from the septum. This should be rather close to an odd multiple of 90 degrees. We shall see that such injection and ejection details often have quite strong influence on the lattice design and should not be left until after the major parameters have been frozen.

One of the problems which arises naturally when the ring is small is that there is not enough room for all the components and this leads to a great shortage of space between the magnets. In Figure 3 we see a typical gap between quadrupole and bending magnet. We must be careful to ensure that their fields do not interfere or, if they do, that we know from measurements with the neighbouring magnet in place, how the effective length of the magnet and quadrupole are affected by the other's presence. We can see in Figure 4 some early measurements of quadrupole gradient along a line parallel to the axis which were made in the 1950's [1], that a steel plate acting as a mirror to simulate the presence of another magnet has a significant effect on the effective length and central field gradient.

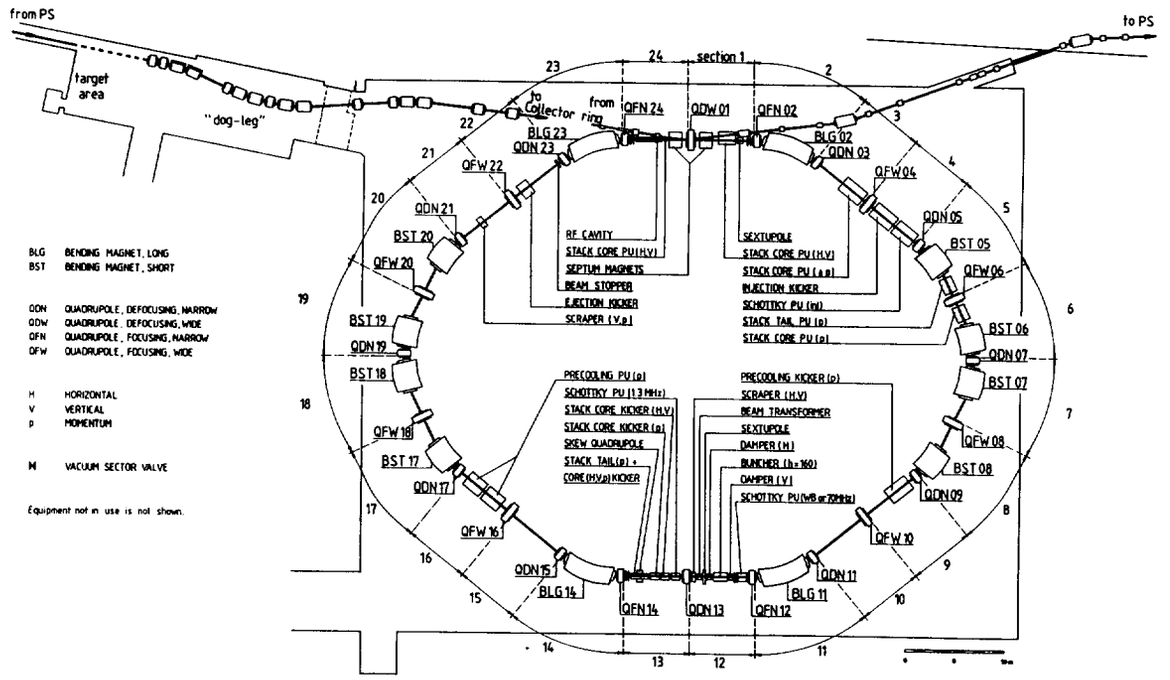

Figure 2: General layout of the Antiproton Accumulator

Figure 3: Gap between a dipole and a quadrupole in the AA.

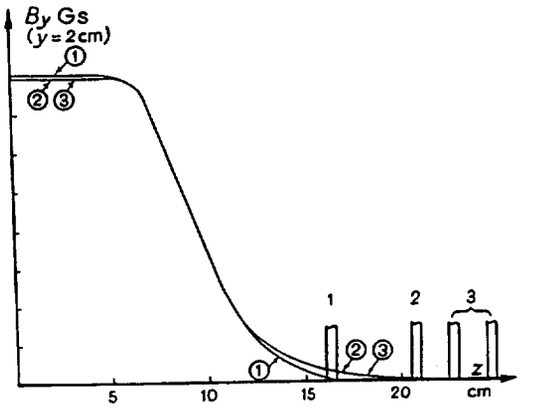

Figure 4: End field shape for a quadrupole with a steel mirror plate

In arriving at a suitable lattice design for this ring we first chose the energy to be 3.5 GeV since this is the energy at which the antiprotons are most abundant and we tried to make the radius 25m, so that its circumference is exactly one quarter of that of the PS. The bunches of protons which produce the antiprotons originate in the PS and it is this machine which will later have to re - accelerate the antiprotons.

It is natural to first try to design around a FODO pattern of quadrupole lenses since this is the simplest from many points of view. Of course, designers of electron rings for synchrotron radiation usually choose another kind of lattice, but the problems we shall discuss tend to be common to any lattice configuration.

This particular ring has a specific requirement imposed by the cooling system which demands that the spread of revolution frequencies, which stems from the momentum spread and which is determined by

$$\eta = \frac{1}{\gamma^2} - \frac{1}{\gamma_{tr}^2} = \frac{p}{f}\frac{df}{dp} , \tag{1}$$

is within rather close limits. This fixes γ_{tr}. Other machine designers will encounter different constraints on this parameter. In high intensity boosters it is often thought a good idea not to include γ_{tr} in the energy range of the synchrotron. In electron rings, although one is far above transition, the momentum compaction which is linked to the energy damping time places a similar constraint on the designer.

The second term in the expression for eta is equal to the momentum compaction function divided by bending radius. It is determined by the change in circumference with momentum about the equilibrium momentum and is just the average value of the dispersion function D(s) around the ring:

$$\frac{1}{\gamma_{tr}^{\ 2}} = \frac{\alpha_0}{R} = \frac{1}{2\pi R}\int \frac{D(s)}{\rho(s)} ds \tag{2}$$

We shall see that this parameter is controlled by the choice of Q value and indeed, for a proton machine transition, is roughly equal to Q. The Q value is in turn closely tied to one quarter of the number of FODO periods since one tries to choose a betatron phase advance of 90 degree or perhaps 60 degrees but rarely outside this range. Since the desired γ_{tr} for the AA was 2.4, the Q was chosen to be 2.3 and therefore the number of periods had to be approximately 10.

If the number of periods is too large the space will be chopped up into too many small pieces; there will be too many components and too many wasteful ends to them. Furthermore, the AA ring has a natural symmetry of four and we are left with only 8, 12 and 16 as possible numbers of periods. When we come to examine the relative merits of the few remaining options we find that N = 8 would suggest a smaller Q value and hence beta, which is roughly R/Q, becomes uncomfortably large. When we considered the acceptance necessary to collect enough antiprotons the apertures of the magnets are large even with N = 12. The larger beta of N=8 would make matters worse. On the other hand 16 periods would result in too many small components.

Once the period number is fixed, the position of all the quadrupoles is determined and the Q value is fixed within narrow limits. The length of the quadrupoles is also determined by the peak field one may allow on their pole pieces which must inscribe an ellipse or rectangle sufficient to accommodate the beam. The lattice functions and the required emittance and momentum spread (100 pi mm. mrad and $\pm$ 3% in the case of the AA) are now pretty well defined and it is merely a matter of juggling to make the exact numbers from a lattice program consistent.

We still have to decide on the layout of bending magnets within the ring and the positions of injection, ejection and (in our example) the cooling systems. The kickers must be 90 degrees (or some odd multiple of this) from the septum and this determines which of the half periods they lie in. The AA ring has a rather special requirement that there will be two "beams" circulating which differ only in momentum as shown in Figure 5, one is the "stack" were antiprotons are accumulated and the other the injected beam which must be physically separated from the stack at the injection kicker. This magnet, which encloses only the injected beam has a movable ferrite shutter which closes the magnet aperture on the stack side to prevent the stack from being disturbed by the firing of the kicker. The two beams must be separated by enough space for this shutter.

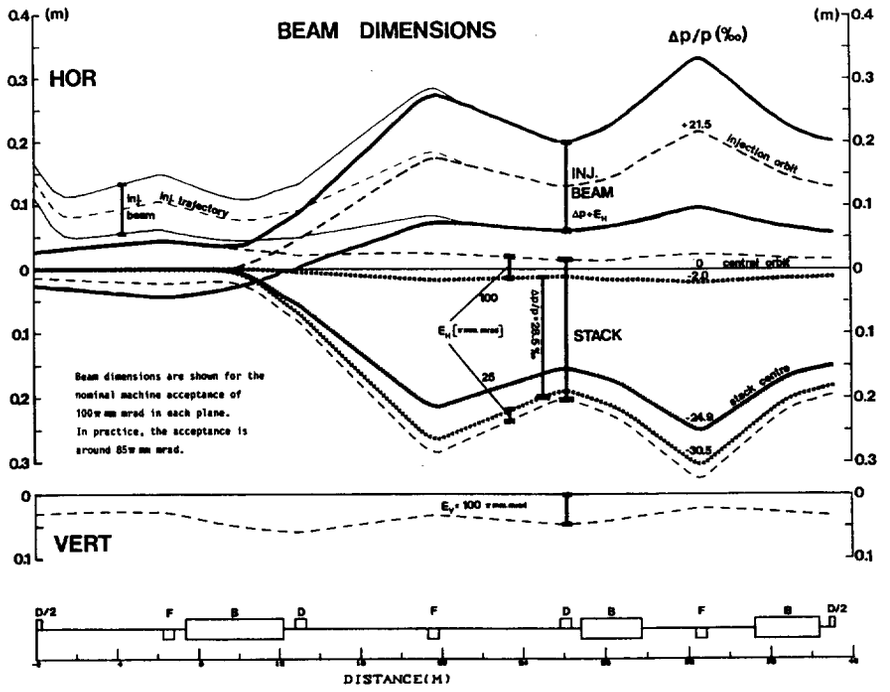

Figure 5: Beam dimensions for one quadrant of the AA.

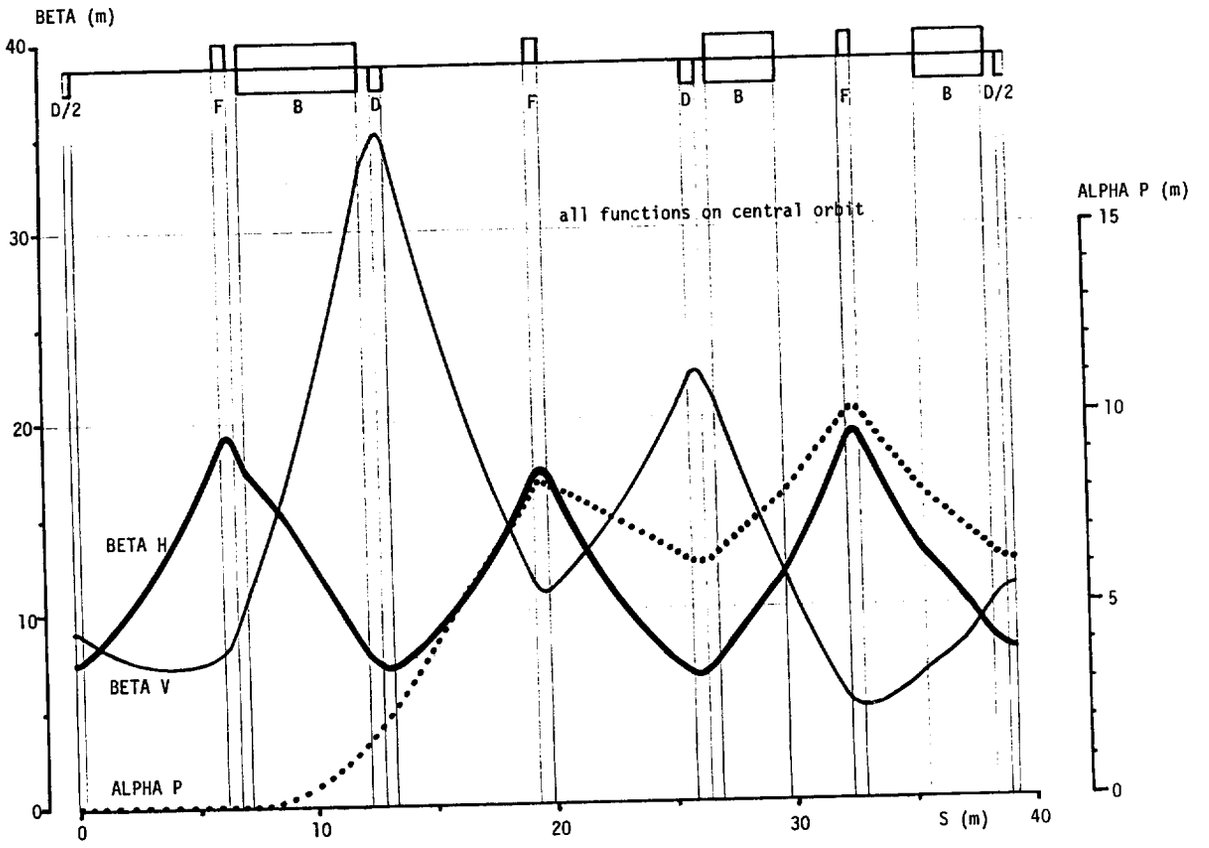

Figure 6: Beta functions and dispersion for one quadrant of the AA.

Elsewhere both beams must pass through a narrow cooling pick - up at 12 and 6 o'clock and there must be a steep rise in the dispersion function between the septum and kicker as can be seen in Figure 6.

This rapid change in dispersion is achieved by choosing to make the lattice symmetric about a D quadrupole at 6 o'clock. We also make use of the horizontal defocusing properties of the end field of a dipole whose faces are tilted horizontally to make an angle with the beam. Both these features help to raise the dispersion as fast as possible immediately after the first dipole encountered by the incoming beam and then cause it to roll over into a high sustained value in the rest of the superperiod [2]. The result is to be seen in Figure 6. I explain this rather peculiar feature only to complete the AA story. Other machines will no doubt have their own special reasons for choosing a particular symmetry or a particular kind of dipole end design.

Once the lattice designer has reached this advanced stage in fixing the design it is high time that he checks with the designers of all the other components of the ring that there is enough room for them to be installed. Some of these will be best placed where the dispersion is zero. In an electron ring this is true of RF cavities and in our example it is the betatron cooling kickers that have this preference. There may be other components, momentum cooling pick - ups in the AA but momentum scrapers in synchrotrons, which need to be where the dispersion is greatest. All these must have enough free length for their function and still leave room for diagnostic pick - ups.

3. MAGNET DESIGN, MEASUREMENT AND CORRECTION

The magnets of small rings tend to be short when measured in numbers of gaps or aperture radii. The end fields of such magnets must be carefully considered because no longer will the shape of the poles in the body of the magnet alone fix the field purity. This is particularly so in the case of the AA magnets which are not only short but have huge apertures in order to accept enough beam Figure 7. Each of the dipoles of a small ring with only a few periods will bend through an appreciable fraction of a circle. In the case of the AA the average entry angle is more than 20 degrees.

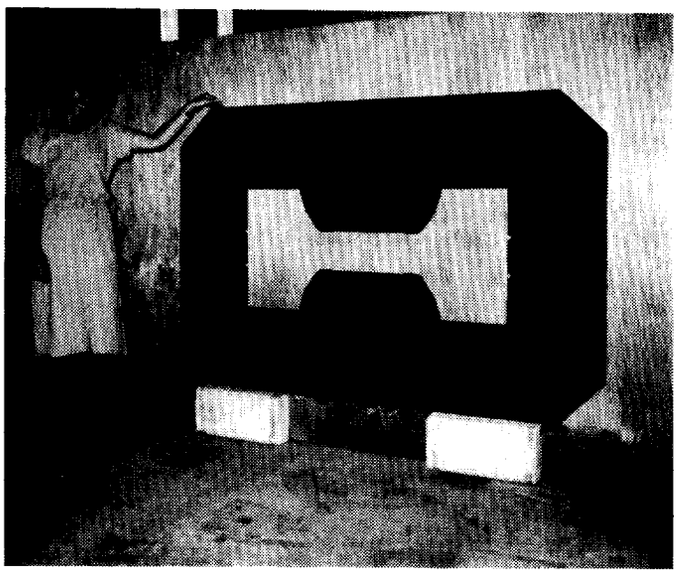

Figure 7: One lamination of an AA dipole magnet

We must decide whether we should make the magnet curved so that the end faces are normal to the entering and exiting beam or whether the magnets will be just simply stacked from parallel laminations so that their ends are parallel and present, in this case, an angle of 20 degrees to the beam. The focusing properties of the two kinds of magnet are quite different. The transport matrices in the horizontal and vertical planes for a magnet which is curved to ensure that the beam enters and leaves normally are given by :

$$M_H = \begin{pmatrix} \cos\theta & \rho\sin\theta & \rho(1-\cos\theta) \\ -\frac{\sin\theta}{\rho} & \cos\theta & \sin\theta \\ 0 & 0 & 1 \end{pmatrix} \tag{3}$$

$$M_V = \begin{pmatrix} 1 & \rho\theta & 0 \\ 0 & 1 & 0 \\ 0 & 0 & 1 \end{pmatrix} \tag{4}$$

We can see that the (2,1) element of the horizontal matrix, which expresses the focusing power, is finite. In contrast, in the vertical plane there is no focusing action. On the other hand you can change this by tilting the end faces by angle ε as shown in Figure 8. To first approximation, the effect of this tilt may be expressed by thin - lens matrices at each end :

$$M_H = \begin{pmatrix} 1 & 0 & 0 \\ \frac{\tan\varepsilon}{\rho} & 1 & 0 \\ 0 & 0 & 1 \end{pmatrix} \tag{5}$$

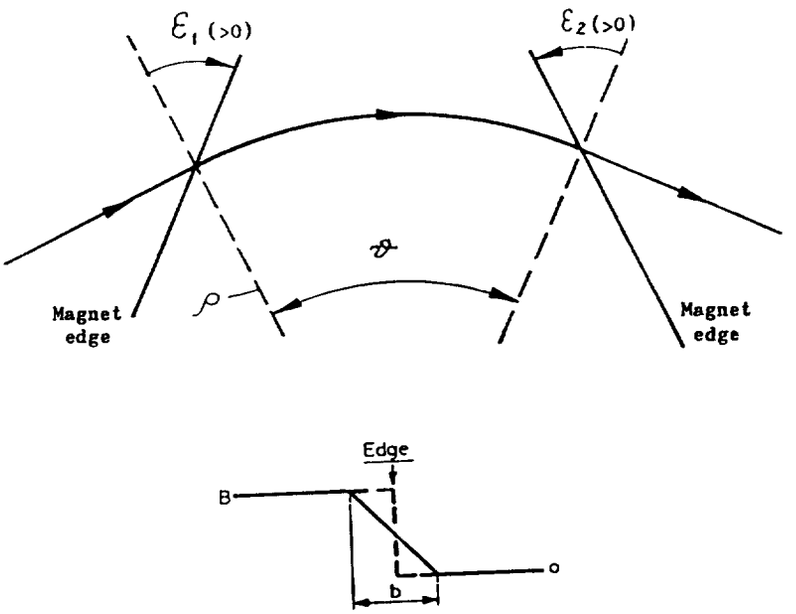

Figure 8: Geometry of a bending magnet which is not a sector.

$$M_V = \begin{pmatrix} 1 & & 1 & 0 \\ \frac{1}{\rho}\left(\frac{b}{6\rho\cos\varepsilon} - \tan\varepsilon\right) & 0 & 0 & \\ 0 & & 0 & 1 \end{pmatrix} \tag{6}$$

For the special case of the parallel ended magnet $\varepsilon = \theta/2$ the (2,1) elements become $\frac{\pm tan(\theta/2)}{\rho}$. If you multiply the matrices together you will find that the focusing power in the horizontal plane is cancelled by these thin lenses and instead, the magnet focuses vertically. Either way one cannot avoid considerable beating of the beta function in one or the other of the transverse phase planes. We see from Figure 6 that we chose to let this happen in the vertical plane of the AA, where apertures were not so huge, rather than adopt complicated special quadrupole arrangements to match it out.

The optical properties are becoming quite precise at this stage and one should recalculate Figure 5 to check aperture dimensions and design the vacuum chamber. We can see that some of the magnets have to house a beam 60 cm wide. This is a very extreme case which illustrates admirably some of the effects which one must be aware of in small ring even if, when calculated for smaller apertures, they prove not to be as important as in the AA.

4. MULTIPOLES IN THE MAGNET DESIGN

One of the difficulties we encounter in an analysis of beam dynamics for such a machine is that there are non - linear terms in the focusing which have to be corrected. These are important for they modify the chromaticity or introduce a variation with momentum in the dispersion of the machine. One must compensate the chromaticity rather precisely in a storage ring and this may be done in a large ring with sets of sextupole magnets. In a small ring there is often too little space for special correction magnets but multipole correction fields may be incorporated in the magnet design. This may

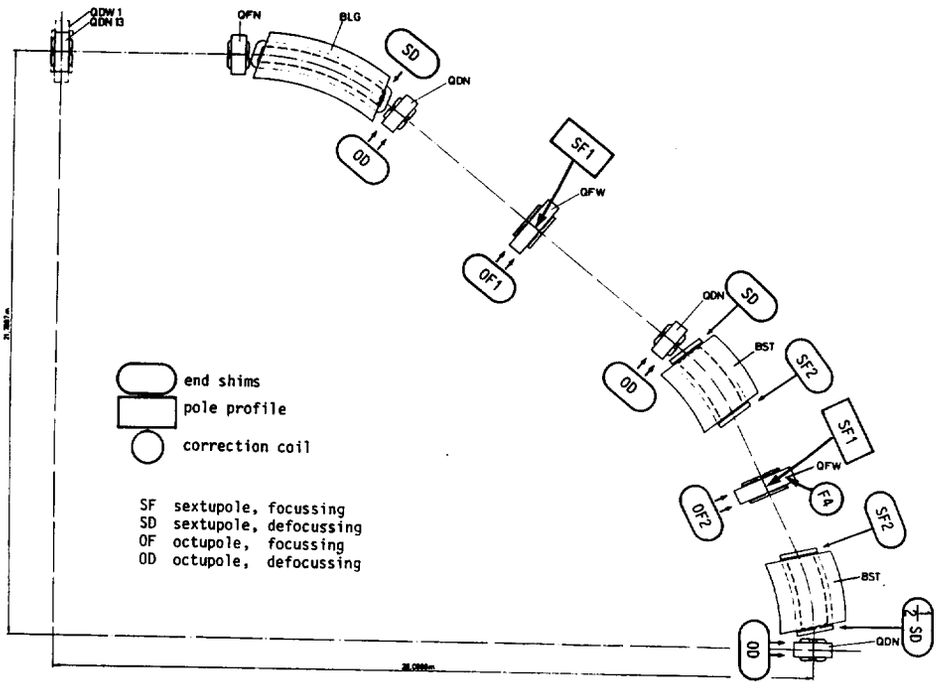

Figure 9: Multipole corrections applied to one quadrant of the AA

either be done by shaping the pole pieces or by shimming their ends with lumps of steel bolted onto the pole pieces. For example we may design the main quadrupoles with poles having a sextupole asymmetry which causes a variation of gradient so that it is no longer the same over the whole width but has a slope so that it is stronger on the outside of the machine and therefore compensates the variation of Q with momentum : the chromaticity. The corrections labelled SF1 in the plan of one quadrant of the AA, Figure 9 are of this type. The left right symmetry of the quadrupole is broken to do this. At the same time any curvature in the variation of Q as a function of momentum may be corrected.

We can see in Figure 10 how the integrated gradient of the quadrupole, designed with a magnet field mesh program, has a linear variation with horizontal displacement plus a quadratic term to match the chromatic curvature. The linear term is sextupolar and the curvature is octupolar (labelled OF, and OD in Figure 9). The same Figure shows correction SF2 and SD which are sextupole terms applied by end shims to the dipoles.

In the AA we designed all these corrections in at the beginning but also provided the means to make adjustments to the radial field variation afterwards with packs of washers mounted on studs protruding from the pole ends. In Figure 11 we see a wide quadrupole magnet being measured and the studs with their washers are clearly seen. The long coil integrates the gradient along a paraxial line. By controlling the number of washers on each stud we can shape the integral of the gradient as a function of horizontal position without using any power or taking up any of the circumference.

In order to calibrate the effect of washers in the 16 different stud positions seen in Figure 12 a pack of six washers was placed on each stud in turn and the change in integrated gradient compared with an unshimmed magnet measurement [3].

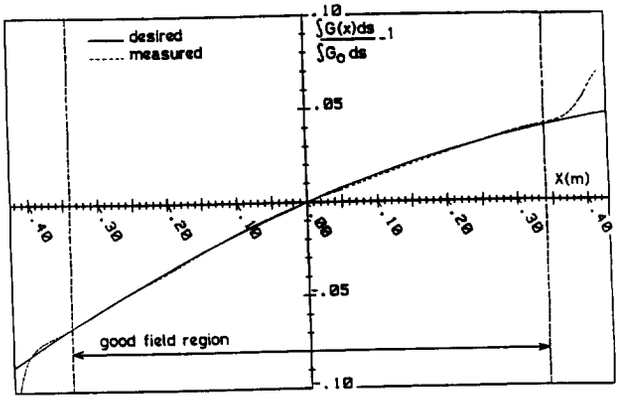

Figure 10: Comparison between required and measured quadrupole gradient

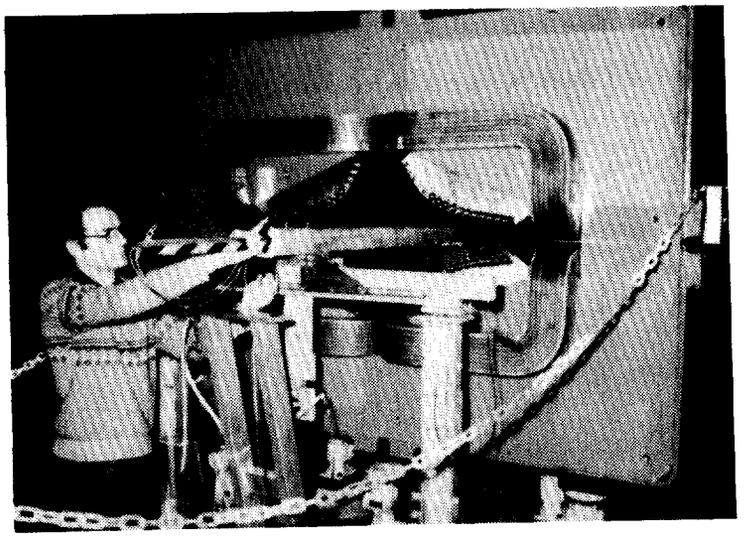

Figure 11: Measurements being made on an AA wide quadrupole

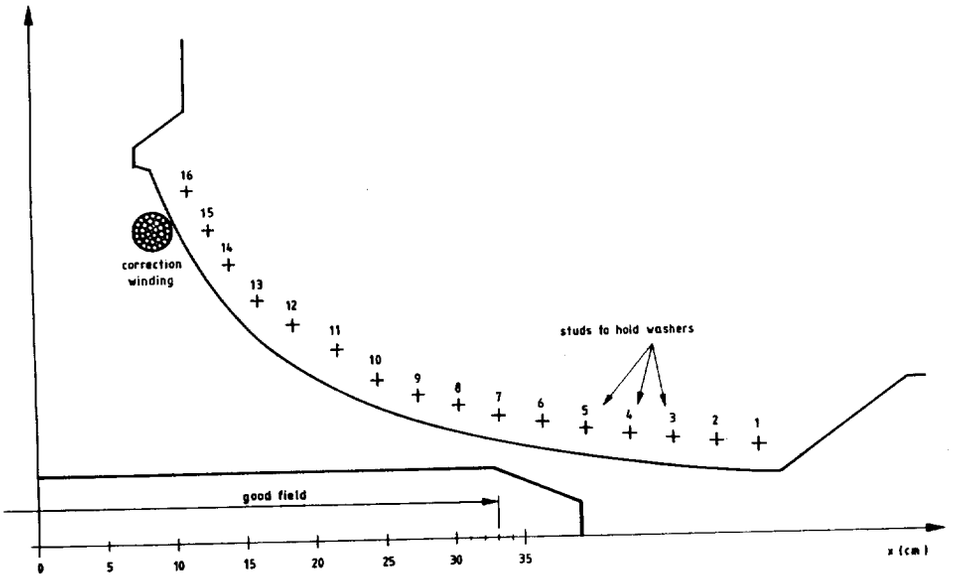

Figure 12: Stud positions and correcting winding on an AA wide quadrupole

The results of this calibration are shown Figure 13 where each curve shows the change in gradient due to one pack of six on each of the washer positions. A program was written to combine combinations of washers to produce any desired change in field gradient.

It proved perfectly practical to shim field shapes empirically on the basis of Q measurements with these washers but the process took several hours. To modify field shapes on - line and with the beam circulating we installed single - turn correction windings which can be seen in Figure 12 mounted on the pole. Their effect was also calibrated by field measurement on a prototype and the results for a range of currents can be seen in Figure 14. Of course such correction windings lead to power supply complications in a pulsed machine

Now we come to consider how successful all this shimming was in correcting the Q variation with momentum. We see in Figure 15 the residual variation in Q when the AA was first switched on [4]. Although every care had been taken there is still a Q variation in the horizontal plane which is larger than the space between the one - third and one - quarter integer resonances.

Adjustments to the end shims were calculated and applied to reduce this by almost an order of magnitude (Figure 16) and when the same points are plotted on a Q_h, Q_v diagram (Figure 17) we find that all sum resonances up to 11th order are avoided. The correction was applied in two iterations.

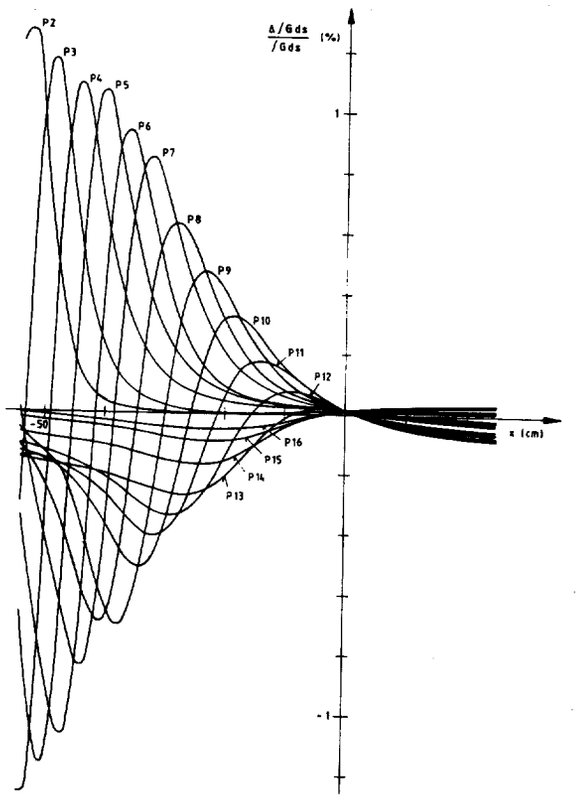

Figure 13: The effect of a six - pack of washers on each stud position

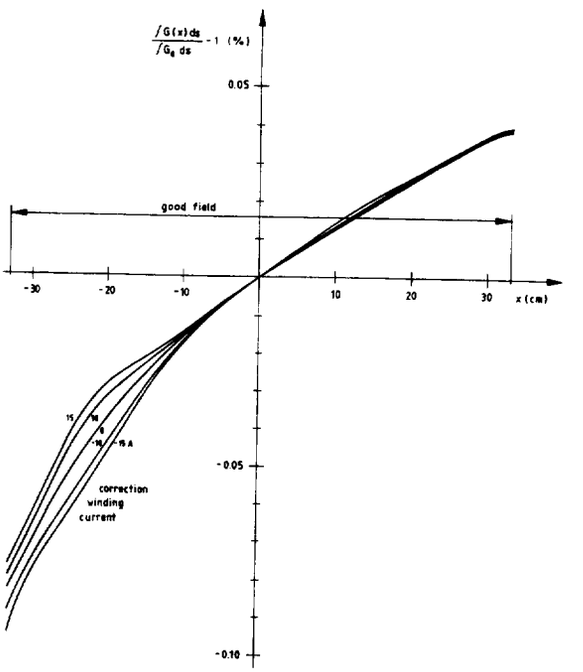

Figure 14: Effect of current in the correction winding of an AA quadrupole

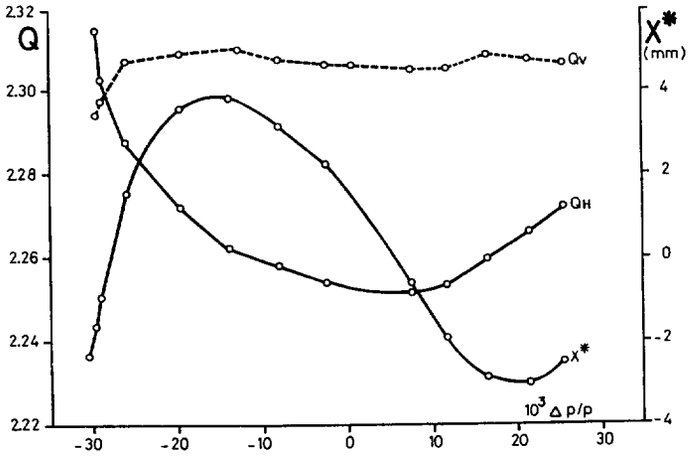

Figure 15: Variation of Q and mid - straight dispersion before correction

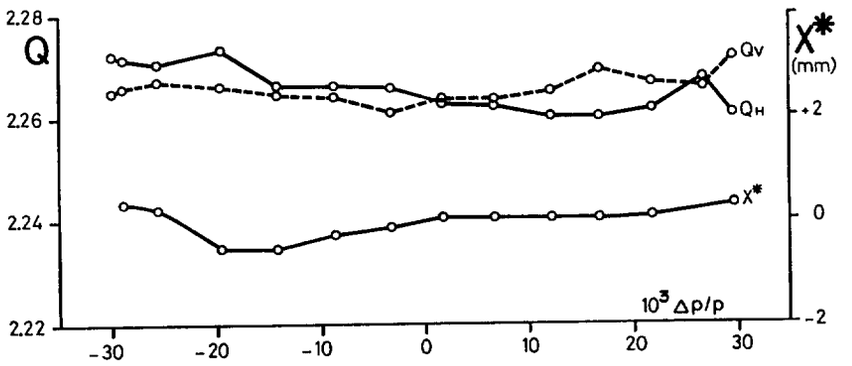

Figure 16: Variation of Q and mid - straight dispersion after correction

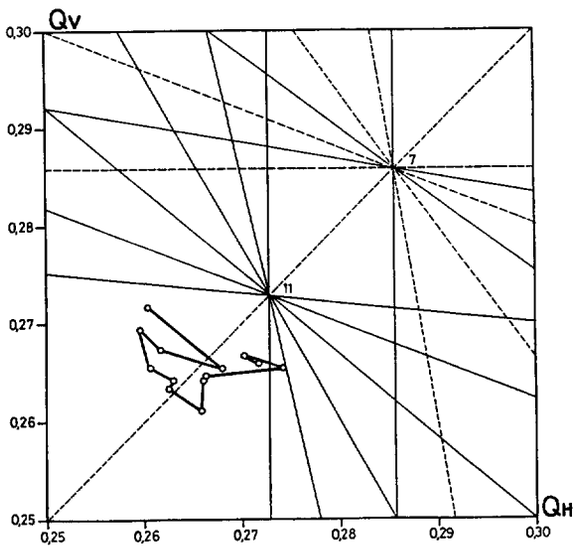

Figure 17: The working line of the AA after correction

5. TWO – DIMENSIONAL FIELD INTEGRALS

And now we should turn to some of the theory behind the description of magnets and how this must be modified when the magnets are only a few gap dimensions long. If a magnet's ends are identical, the field in the plane of symmetry mid way between the ends will be "two dimensional". Symmetry dictates that there can be no axial component, B_y. Laplace's equation for the scalar magnetic potential, ϕ :

$$\frac{\partial^2\phi(x,y,z)}{\partial x^2} + \frac{\partial^2\phi(x,y,z)}{\partial y^2} + \frac{\partial^2\phi(x,y,z)}{\partial z^2} = 0 \tag{7}$$

reduces to just the outer two terms [5]. The two - dimensional equation has the very attractive property that the solution is a harmonic series

$$\phi = \phi_n r^n \sin(n\theta) \ . \tag{8}$$

Each term in this series corresponds to a magnet with a different number of poles. The index n of the n'th term is just half the number of poles. pure multipole would have which produced the n'th term in the series. It is also associated with the order of the non - linear resonance which this multipole can produce. For example if n is 2 we obtain the field produced by a quadrupole. The potential must reverse as we describe a circle of constant radius to have two positive and two negative excursions corresponding to the four poles. Of course, in this case, the motion is linear and any resonant condition has order 2.

This is a useful simplification when we consider the dynamics of a beam passing through a long magnet where most of the field has this two - dimensional property. We can even preserve this simplification when we include the end fields of a short magnet provided the deflection in the magnet is small, as is the case in high energy synchrotrons with large radius. We can then approximate the particles equilibrium orbit to a straight line paraxial to the centre line of the magnet. The integral of the potential along such a line, in other words, the average potential, has the same two - dimensional properties. This may be proved by integrating the three terms of Laplace equation along such a line. The middle term becomes:

$$\int_{-y_0}^{y_0} \frac{\partial^2\phi(x,y,z)}{\partial y^2} dy = \left[\frac{\partial\phi(x,y,z)}{\partial y} \right]_{-y_0}^{y_0} \tag{9}$$

Clearly if y_0 is taken arbitrarily far away from the ends the expression will be zero at each limit. Each of the other two terms becomes a simple average of the transverse second derivatives of potential. For example:

$$\int_{-y_0}^{y_0} \frac{\partial^2\phi(x,y,z)}{\partial z^2} dy = \frac{\partial^2}{\partial z^2}\left[\frac{1}{2y_0} \int_{-y_0}^{y_0} \phi(x,y,z) dy \right] = \frac{\partial^2\overline{\phi}}{\partial z^2} \tag{10}$$

and the two - dimensional Laplace Equation as well as its trigonometrical solutions apply exactly to the averages of the potential along paraxial lines. The average transverse fields seen by the particles are just the derivatives of the average potential and are the familiar trigonometric series with n being half the number of poles in the multipole associated with each term.

It is of course the vector potential, **A**, which is more commonly used in the study of beam dynamics since it describes the effect of magnetic field in the Hamiltonian of the motion. In the two - dimen-

sional case A_x and A_z are zero and the axial component obeys Laplace's equation in two - dimensions producing a harmonic series solution for the field expansion.

The two - dimensional solution of A_y may also be expressed in Cartesian coordinates as a polynomial:

$$A_y = \sum_{1}^{\infty} A_n f_n(x,z) \tag{11}$$

where :

$$f_n(x,z) = (x + iz)^n \quad . \tag{12}$$

For a quadrupole this is:

$$f_n(x,z) = (x^2 - z^2) + i(2xz) \quad . \tag{13}$$

We can derive the transverse field components:

$$B_z = \frac{\partial A_y}{\partial x} = \sum_{1}^{\infty} n A_n x^{(n-1)} \tag{14}$$

when z = 0 . And we can deduce that the imaginary terms in the polynomial correspond to the skew orientation of multipoles while the real term in our example could represent a normal lattice quadrupole. A real cubic term would be a sextupole with a vertical plane of symmetry while the imaginary cubic terms stem from a skew sextupole, one that is, which has been rotated about its axis by 1/12 of a revolution.

We find, therefore that there is a simple association between the terms in the Cartesian expansion and the order of multipole, just as there was in the polar case. We can even go further to associate each term with a term in the Taylor expansion of the field about the axis of the magnet:

$$B_z = \sum_{1}^{\infty} \frac{1}{(n-1)!} \frac{dB^{(n-1)}_z}{dx^{(n-1)}} x^{n-1} \tag{15}$$

and thus a quadrupole produces a gradient, a sextupole a second derivative and higher multipoles produce successively higher derivatives.

All of this applies equally to particles whose path may be approximated by paraxial rays and to measurements made with long paraxial search coils which extend clear of the magnetic field at each end. One can often identify the multipole content of the magnet simply by inspecting the transverse dependence of the field measured by such a coil. A quadratic variation indicates a sextupole and a cubic points to an octupole error term.

Just to complete this two - dimensional treatment, which I repeat is an approximation valid only for paraxial trajectories, let us recall the simple Hamiltonian:

$$H = \frac{p_x^2}{2} + \frac{p_z^2}{2} - \left(\frac{e}{p}\right) A_s \quad . \tag{16}$$

The vector potential term can, in the paraxial approximation , be written:

$$A_s \approx \sum_{1}^{\infty} A_n f_n(x,z) \tag{17}$$

and we can conveniently associate each multipole with a term in the Hamiltonian. So for our example of a quadrupole we obtain for the motion in the x direction:

$$H = \frac{p_x^2}{2} - \frac{kx^2}{2} \tag{18}$$

where k is the normalized gradient $B'/(B\rho)$. Application of Hamilton's equations leads rapidly to the familiar Hill's equation of motion. This is using a sledgehammer to crack a nut but when we come to introduce higher order terms which are non - linear the power of the Hamiltonian produces an overall simplification.

6. CURVILINEAR COORDINATES

The above treatment is all well and good for large synchrotrons but breaks down seriously if the dipoles of the ring bend particles significantly from a paraxial path. This is much more likely to be the case in a small ring with a few focusing periods. In such a case we may consider a model which I will refer to as the "sliced loaf" model in which the end field is broken up into elementary slices each of which may be represented as one of the multipole shaped fields of the two - dimensional model. We would expect such a model to be capable of telling use, for instance, how bad the effect of correcting an error in the field due to the pole profile by putting shims on the end of the magnet. The two fields would not quite compensate for a particle that moved its position with respect to the magnet axis as it entered the fringe field.

To make this model work we must be very careful with the curvature of the trajectory. Bengtsson [6] has recently made an elegant analysis of this using the metric tensor which defines the relation between differential changes in the curvilinear system to the rectilinear Cartesian system:

$$g_{\mu\nu} = \begin{pmatrix} 1 & 0 & 0 & 0 \\ 0 & -1 & 0 & 0 \\ 0 & 0 & -(1+hx)^2 & 0 \\ 0 & 0 & 0 & -1 \end{pmatrix} \tag{19}$$

where h is the curvature $1/\rho$. Using the four - vector coordinates of special relativity he arrives at a differential equation of motion:

$$\frac{d^2x^\mu}{d\tau^2} + \Gamma^\mu_{\nu\lambda}\frac{dx^\nu}{d\tau}\cdot\frac{dx^\lambda}{d\tau} = \frac{e}{m_0c^2}F^\mu{}_\nu\frac{dx^\nu}{d\tau} \tag{20}$$

where $F^\mu{}_\nu$ is the electromagnetic field tensor.This is really just an up - market version of:

$$\frac{d^2x}{dt^2} = \frac{e}{m_0}\ \mathbf{v}\times\mathbf{B} \tag{21}$$

and we can see that the middle extra term contains all the information on the transformation to curvilinear coordinates. He derives explicit equations of motion from this expressed in terms of the two - dimensional harmonic field coefficients. Later he derives a Hamiltonian in terms of the normalized quadrupole and sextupole strengths, k and m, and including the effect of dispersion, D, on a particle with a momentum defect $\delta = dp/p$:

$$
\begin{aligned}
H = & \frac{1}{2}\{h^2 - k - \delta[(m + 2hk)D + h^2 - k]\}x^2 \\
& + \frac{1}{2}\{k + \delta[(m + hk)D - k + h'D']\}z^2 \\
& - \frac{1}{6}(m + 2hk)x^3 + \frac{1}{2}(m + hk)xz^2 \\
& + \frac{1}{2}(1 + \delta hD)p_x^2 + \frac{1}{2}(1 + \delta hD)p_z^2 \\
& + \delta hD'xp_x + \frac{1}{2}h'z^2p_x + \frac{1}{2}hxp_x^2 + \frac{1}{2}hxp_z^2
\end{aligned}
\tag{22}
$$

Inspecting this Hamiltonian we first should note the appearance of the focusing strength, k, alone in the first two lines. This is just like the simple two - dimensional Hamiltonian from which one may derive linear betatron motion. We can see that the focusing will be modified by the first term h^2. This term will be familiar to those who remember combined function machines. The square brackets in the first two lines contain terms which affect the off - momentum behaviour. The simple focusing terms k and h^2 appear again here to express chromaticity. The sextupole strength, m , also appears as a coefficient of δD and this must describe the effect of sextupoles in modifying the chromaticity. Terms which contain the product, hk, must be peculiar to combined function lattices where curvature and focusing occur in the same element but we should not ignore the product $h'D'$ in the second term which tells us that the shape of the curved orbit can modify vertical chromaticity.

Turning to the third line we have two terms which, in a separated function lattice in which hk = 0 just describe the effect of sextupoles on the betatron motion. These terms occur in our simple two - dimensional description. One can derive the strength of non - linear resonances from these terms. The fourth and fifth lines contain momentum dependent terms in which the curvature, h, is present and the last three terms which modify the betatron motion for on momentum particles where there is finite curvature and, presumably can contribute to non - linear resonance width.

If we follow the analysis of the "sliced bread" model of Bengtsson and which is also embodied in computer programs like ORBIT [7], MAD [8], we go a long way towards an exact description of the end field of magnets. The lattice functions, dispersion and chromaticity will turn out close to reality. However there remains one more effect which is less well known and which to the best of the author's knowledge is correctly embodied in only one computer program MIRKO [9]. We shall call it Electron Microscope Distortion since it is well known in that field.

7. EXCURSIONS WITHIN THE END FIELD

Suppose we return to the model of paraxial trajectories and ignore curvature for the moment. We have shown that the integrated field is two - dimensional but we know that locally this is not the case. The paraxial particle may see, say, a left hand deflecting field from the three dimensional nature of the field as it enters the end field region but our paraxial theorem tells us this is exactly cancelled by an equal and opposite right hand deflection somewhere else in the end field. Now suppose the particle is following a line which is not paraxial because the beta function is varying in the end field or perhaps it is an off - momentum particle whose displacement follows the dispersion function and is not therefore paraxial. The two perturbations will now be different because the paraxial theorem relies on the particle staying the same distance from the axis through the end field and this is no longer the case. In order

to understand such effects we must have a model for the end field which expresses how the multipole coefficients vary as a function of distance along the beam axis. There is a complete polynomial expression for the three - dimensional end field to be found in a text by Glaser on electron optics [10] and we reproduce this polynomial for the scalar potential as he wrote it.

$$\begin{aligned}\varphi_m(x,y,z) = \Phi_m &- Gx - Hy - \tfrac{1}{4}(\Phi_m'' - \Delta)x^2 + Qxy - \tfrac{1}{4}(\Phi_m'' + \Delta)y^2 \\ &+ \tfrac{1}{3}(\tfrac{1}{2}G'' + G_1)x^3 - H_1x^2y - G_1xy^2 + \tfrac{1}{3}(\tfrac{1}{2}H'' + H_1)y^3 \\ &+ (\tfrac{1}{64}\Phi_m^{(4)} - \tfrac{1}{48}\Delta'' + \Delta_1)x^4 - (\tfrac{1}{12}Q'' - 4Q_1)x^3y \\ &+ (\tfrac{1}{32}\Phi_m^{(4)} - 6\Delta_1)x^2y^2 - (\tfrac{1}{12}Q'' + 4Q_1)xy^3 \\ &+ (\tfrac{1}{64}\Phi^{(4)} + \tfrac{1}{48}\Delta'' + \Delta_1)y^4 .\end{aligned} \tag{23}$$

The coefficients G, H, Q refer to vertical and horizontal dipole and quadrupole fields respectively. Other coefficients contain the axial derivatives of these quantities. We can still identify most of the multipole coefficients although in Glaser's notation we must remember that x and y are transverse and z is axial.

Table 1

Terms in Glaser's expansion according to multipole symmetry

NAME	φ_m	B_y	B_x	dB_y/dx	dB_x/dy
SOLENOID	$\phi_m - \phi''r^2/4 + \phi^{(IV)}r^4/64$	$-\phi^{(IV)}(x^2y + y^3)/16$	$-\phi^{(IV)}(y^2x + x^3)/16$	$-\phi^{(IV)}xy/8$	$-\phi^{(IV)}xy/8$
H BENDING	$-Hy$	H	0	0	0
V BENDING	$-Gx$	0	G	0	0
QUADRUPOLE	Qxy	$-Qx$	$-Qy$	$-Q$	$-Q$
SKEW QUADRUPOLE	$\Delta(x^2 - y^2)/4$	$\Delta y/2$	$-\Delta x/2$	0	0
SEXTUPOLE	$H_1(y^3 - 3x^2y)/3$	$H_1(x^2 - y^2)$	$2H_1xy$	$2H_1x$	$2H_1x$
SKEW SEXTUPOLE	$G_1(x^3 - 3xy^2)/3$	$2G_1xy$	$G_1(y^2 - x^2)$	$2G_1y$	$2G_1y$
OCTUPOLE	$\Delta_1(x^4 - 6x^2y^2 + y^4)$	$4\Delta_1(3x^2 - y^3)$	$4\Delta_1(3xy^2 - x^3)$	$24\Delta_1xy$	$24\Delta_1xy$
SKEW OCTUPOLE	$4Q_1(xy^3 - x^3y)$	$4Q_1(x^3 - 3xy^2)$	$4Q_1(3x^2y - y^3)$	$12Q_1(x^2 - y^2)$	$12Q_1(x^2 - y^2)$
END QUADRATIC	$(G''x^3 - H''y^3)/6$	$H''y^2/2$	$-G''x^2/2$	0	0
END CUBIC	$-Q''(x^3y + xy^3)/12$	$Q''(x^3 + 3xy^2)/12$	$Q''(3x^2y + y^3)/12$	$Q''(x^2 + y^2)/4$	$Q''(x^2 + y^2)/4$

In Table 1 we can see the same terms sorted according to the familiar multipoles and shown in the various columns are the expression for the fields and their gradients. Near the bottom of the table are two lines which we name "end quadratic" and "end cubic" which do not fit into our multipole description. The "end cubic" looks at first sight like an octupole but when its field gradient or focusing effect is plotted as a function of the transverse (x, y) in Figure 18 we see it is like a hammock while an octupole Figure 19 is a saddle shape. Anyone who has tried to sleep in a saddle or ride in a hammock will avow to the different topology of these functions.

If we look carefully at the symmetry of the end field cubic we find that while it has the symmetry of a quadrupole in θ its radial dependence is that of an octupole. It is a characteristic of the end field of a quadrupole and proportional to the slope of the main gradient term, Q. Such terms must be included explicitly in any simulation of the end field shape although their effect in one plane can be thought of as a simple multipole.

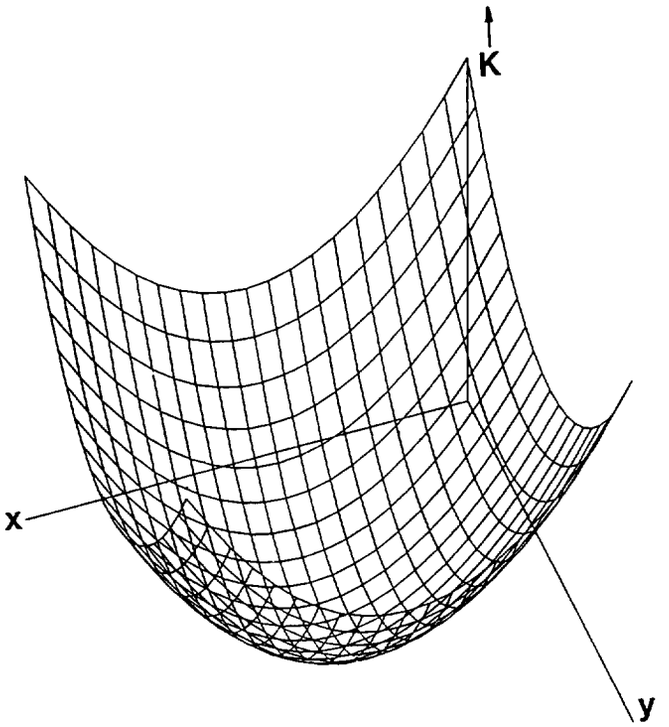

Figure 18: End quadratic potential.

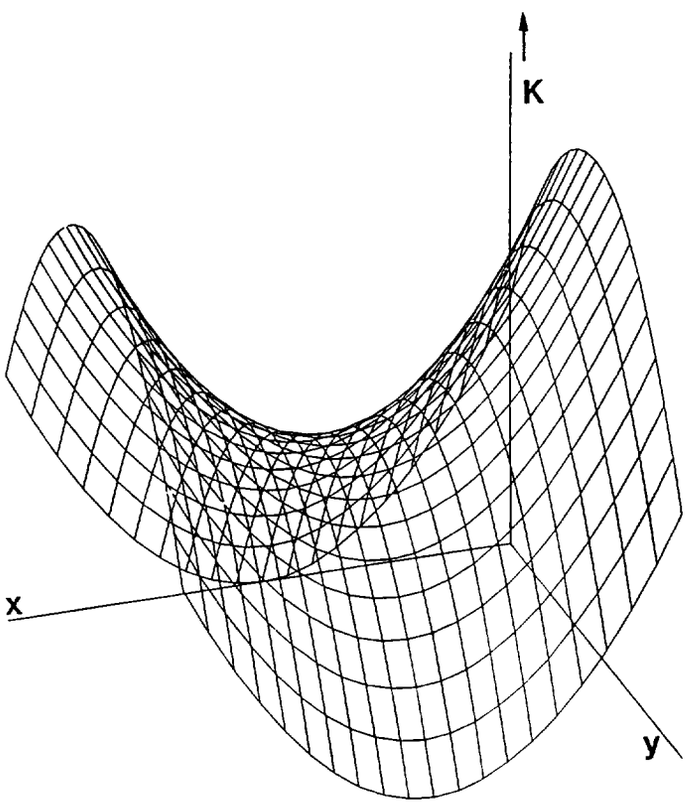

Figure 19: Octupole potential.

Because Q' reverses sign as we pass through the fringe field the paraxial integral of these terms is zero but they have an effect which is proportional to the slope of the betatron function, α, and, in the case of an off - momentum particle, to the slope of the dispersion function [11].

At the time that the AA ring was designed this effect had not been discovered and it is still not incorporated in the standard lattice programs. When it was simulated with the MIRKO program, it exactly matched the curvature in Q versus momentum (Figure 15) before empirical shim correction was applied. Simulation has also shown that it can drive fourth order resonances. Clearly both of these effects become significant only in small rings of short magnets where the emittances and momentum spread are large.

8. CONCLUSIONS

In this review of the special features of small rings we have re - examined some of the approximations which are normally built into the analysis and the computer programs which describe transverse motion in today's large synchrotrons. The accelerator designer should be particularly careful of these approximations when the ring he is designing has magnets which bend through an angle of a few degrees or when the magnet length, measured in number of gap widths, is small.

The practical problem of having so many ends of quadrupoles, dipoles and other equipment in a small ring yet finding enough room for the components themselves is always severe but can be made less difficult if corrections are built into the magnet design and tuned by modifications to the ends of poles. One may even save the space for closed orbit dipoles by installing remotely controlled jacks to support the quadrupoles. This solution proved perfectly successful in the design of the AA and later the Antiproton Collector ring.

Finally, although there has been no time in this review to apply these lessons to small electron ring, many of the considerations are equally valid [13]. However the reader can readily appreciate that some of the correction methods may not be possible in a fast cycling electron ring and the acceptances may not be large enough for the finer points of the end field shape to be an important consideration. Nevertheless, the scenario for the design of the AA is a good vantage point to scan the horizon of possible pitfalls.

* * *

REFERENCES

1. Grivet and Septier. *Les Lentilles Quadrupolaire Magnetiques* CERN 58 – 25

2. B.Autin *Dispersion Suppression with Missing Magnets in a FODO Structure Application to the CERN Antiproton Accumulator* Proceedings of the 1979 Particle Accelerator Conference, San Francisco, IEEE Transactions on Nuclear Science Vol.NS – 268,No.3,pp.3493 – 5,(1979)

3. R.Brown,T.Dorenbos,M.Frauchiger,C.D.Johnson,L.Petty *An Automated Measuring System for the Antiproton Accumulator Magnets* Proceedings of the 7th. International Conference on Magnet Technology, Karlsruhe,IEEE (1981)

4. B.Autin,R.Billinge,R.Brown,G.Carron,C.Johnson,E.Jones, H.Koziol,C.Leeman,T.R.Sherwood,S.van der Meer,E.J.N.Wilson *Beam Optics Studies on the Antiproton Accumulator* Proceedings of the 1981 Particle Accelerator Conference, Washington, IEEE Transactions on Nuclear Science Vol.NS – 28,No.3,pp.2055 – 7,(1981)

5. W.C.Elmore and M.W.Garret *Measurement of Two - Dimensional Fields. Part1:Theory* Review of Scientific Instruments, Vol 25, No.5 ,pp.482 – 483 (1954)

6. J.Bengtsson *Non - Linear Transverse Dynamics for Storage Rings with Applications to the Low - Energy Antiproton Ring (LEAR) at CERN* CERN 88 – 05

7. B.Autin and M.Bell *ORBIT – A Computer Program for Circular Machines* Users Guide (available from authors, CERN,Geneva)

8. F.C.Iselin and J.Niederer *The MAD Program – Users Reference Manual* CERN LEP – TH 88 – 38

9. B.Franczak *MIRKO – An Interactive Program for Beam Lines and Synchrotrons* Computing in Accelerator Design and Operation, Lecture Notes in Physics No.215 p.170 ,pub: Springer Verlag (1974)

10. W.Glaser *Elektronen &hyph und Ionenoptik* Handbuch der Physik, Band XXXIII,Springer Verlag (1956),p.166.

11. E.J.N.Wilson *Strange Multipoles in Magnet Ends* CERN PS/ACOL/Note 84 – 3

12. P.Krejcik *Non - Linear Quadrupole End - Field Effect in the CERN Antiproton Accumulator* Proceedings of the 1987 IEEE Particle Accelerator Conference, Washington, IEEE Catalog No. 87C#2387 – 9,pp.1278 – 9

13. J.P.Delahaye,A Krusche *The Lattice Design of the LEP Electron Positron Accumulator (EPA)* Proceedings of the 1983 Particle Accelerator Conference, Santa Fe, IEEE Transactions on Nuclear Science, Vol NS – 30,No.4,(1983),p.2050